

Supporting Information

Studies of chain substitution caused sub-fibril level differences in stiffness and ultrastructure of wildtype and oim/oim collagen fibers using multifrequency-AFM and molecular modeling

Tao Li,^{1,†} Shu-Wei Chang,^{2,3} Naiara R. Florez,⁴ Markus J. Buehler,³ Sandra Shefelbine,^{5,} Ming Dao,^{6,*} and Kaiyang Zeng^{1,*}*

¹Department of Mechanical Engineering, National University of Singapore, Singapore.

²Department of Civil Engineering, National Taiwan University, Taipei 10617, Taiwan.

³Department of Civil and Environmental Engineering, Massachusetts Institute of Technology, Cambridge, MA, USA.

⁴Department of Bioengineering, Imperial College London, London SW7 2AZ, UK.

⁵Department of Mechanical and Industrial Engineering, Northeastern University, Boston, MA, USA.

⁶Department of Materials Science and Engineering, Massachusetts Institute of Technology, Cambridge, MA, USA.

Note 1.

Dual-frequency AFM method: AM-FM is a typical dual-frequency AFM technique and was used to observe the stiffness distribution of the collagen fibers. It uses two different eigenmode frequencies, the fundamental eigenmode is driven by the amplitude-modulation (AM) technique, while a higher eigenmode is driven by the frequency-modulation (FM) technique. The higher eigenmode is very sensitive to tip-sample interactions that varies with the material properties during imaging, so that the stiffness mappings along single collagen fiber can be quantified. A phase-locked loop (PLL) is included in the control loop for the frequency-modulation. The PLL continuously measures the instantaneous frequency of the oscillation signal and generates an excitation signal at this frequency as a feedback to the control loop. It maintains a 90° phase difference between the response and drive, and thus ensures that the cantilever eigenmode always oscillates at its actual resonance frequency [1]. The PLL can operate in two different modes: constant excitation (CE) and constant amplitude (CA). CE mode keeps the excitation amplitude constant, while CA mode keeps the oscillation amplitude constant by adjusting the drive amplitude accordingly [1]. In case of the CA mode that was used in this work, the frequency shift and drive amplitude are directly related to the conservative and dissipative tip-sample interactions, respectively [2]. FM provides two types of data, the frequency and drive amplitude. The frequency image can be further converted to tip-sample contact stiffness (N/m) with proper calibration of the cantilever, or to elastic modulus (Pascal) through the contact mechanics models (not included in this work). Different from nanoindentation techniques, AM-FM is a tapping mode-based AFM technique that only characterizes the surface layer of collagen fibers instead of the bulky property. Applied force is small enough to prevent any permanent damage of the fibers. The superior resolution of AM-FM is achieved by the intrinsic tapping mode mechanism, in which the contact radius (r) is approximately 3~5 nm based on the classical contact mechanics theory $r = (R \times d)^{1/2}$ (R : tip radius is 8 ± 2 nm, d : indentation depth, and tip wear should be minor due to the higher tip hardness and stiffness than those of the collagen fibers). As the primary usage of the AM-FM in this work is to quantify the elasticity mapping, it has to operate in the repulsive regime to achieve certain indentation depth (usually a few nanometers) to the sample surface. Hence, the drive voltage is set to be 2 V for the fundamental eigenmode, and 10 mV for the third eigenmode. This small amplitude of FM mode prevents the perturbation to the first eigenmode cantilever dynamics and ensure the cantilever oscillates at the repulsive regime (phase $< 90^\circ$). The probes used here are the same as the one for AFM imaging (PPP-FM, Nanosensors, Switzerland). The cantilever stiffness and sensitivity of every probe used for AM-FM imaging were calibrated using the same method as described in the main text.

<i>Specifications</i>	<i>Values</i>
1st eigenmode resonance frequency, kHz	80~90
3rd eigenmode resonance frequency, MHz	1.5
1st eigenmode InvOLS,^{a)} nm/V	70~130
1st eigenmode stiffness k, N/m	3~4
Tip radius of curvature, nm	8±2
Cantilever dimension (L, W, H), μm	225, 28, 3
Coatings, tip and cantilever	None

a) InvOLS: inverse optical lever sensitivity

Table S1. Typical calibrated specifications of AFM probe (PPP-FM, NANOSENSORS, Switzerland).

Note 2.

Statistical analysis of morphology features of WT and *oim/oim* collagen fibers:

Directly viewed from Figs. 2A and 2B, the *+/+* collagen fibers are wider than the *oim/oim* ones. By averaging 16 fibers for each type of bone, the diameter of *+/+* fibers is found to be 177.50 ± 52.79 nm, whereas the diameter of *oim/oim* fibers is 82.50 ± 17.33 nm, which is reduced by 54% of the mean diameter of the *+/+* fibers ($p < 0.001$). The smaller value of standard deviation may indicate the less heterogeneity of *oim/oim* fibers. Such significant diameter reduction of the homozygous *oim/oim* collagen fibers was also reported by Weis et al., based on the study from mice hearts [3]. The diameter reduction can be a universal feature of different types of organs or tissues in *oim/oim* mice.

Based on the histograms distributions (Fig. 2C), the highest number of count for the D-spacing in *oim/oim* fibers is at 67 nm, while for *+/+* fibers it is between 70 and 71 nm. The ranges of D-spacing distributions for both type of collagen fibers are similar, except that a few *+/+* fibers show diverged D-spacing (75 nm) than the others. Statistical analysis (one-way ANOVA) was conducted based on the D-spacing measurements from 33 collagen fibers respectively for both *+/+* and *oim/oim* bones. For all evaluations, a value of $p < 0.05$ is considered significant. The homogeneity of variance by Levene's test indicates that the population variances are not significantly different ($p = 0.271$). The graph of cumulative distribution function (CDF) (Fig. 2D) demonstrates the shift of the entire population of *oim/oim* fibers towards the lower D-spacing values comparing to that of the *+/+* fibers. Fig. 2E also demonstrates such difference, and the large offset between the maxima and the 95% data range for *+/+* fibers is attributed to the occasionally observed fibers with exceptionally large D-spacing. Generally speaking, the air-dried mineralized *+/+* collagen fibers have significantly larger diameter and D-spacing than those of *oim/oim* fibers. The shorter D-spacing of *oim/oim* fiber is also supported by the result from the molecular simulation (Fig. 3). This simulation showed that the *oim/oim* collagen fibril has 2~5% shorter D-spacing. It also demonstrated a larger gap region and shorter overlap region of *oim/oim* fibril when compared with normal collagen fibril. This result is also consistent with the measurement from the AFM morphology, in which the *oim/oim* fibers also show wider gap zones than that of the *+/+* fibers.

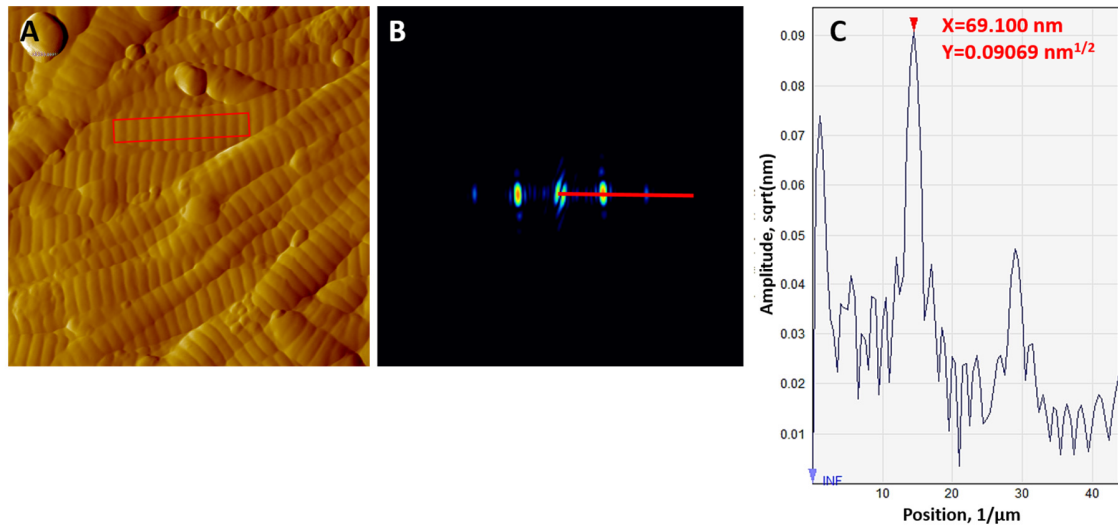


Figure S1. Example of D-spacing observation by 2D-FFT (SPIP software, Image Metrology, Denmark) on +/- collagen fibers. (A) AFM amplitude image. Red rectangle is the interested area. (B) 2D-FFT patterns for the interested area. (C) Profile along the red line in (B), showing the D-spacing value of 69.1 nm at the highest peak.

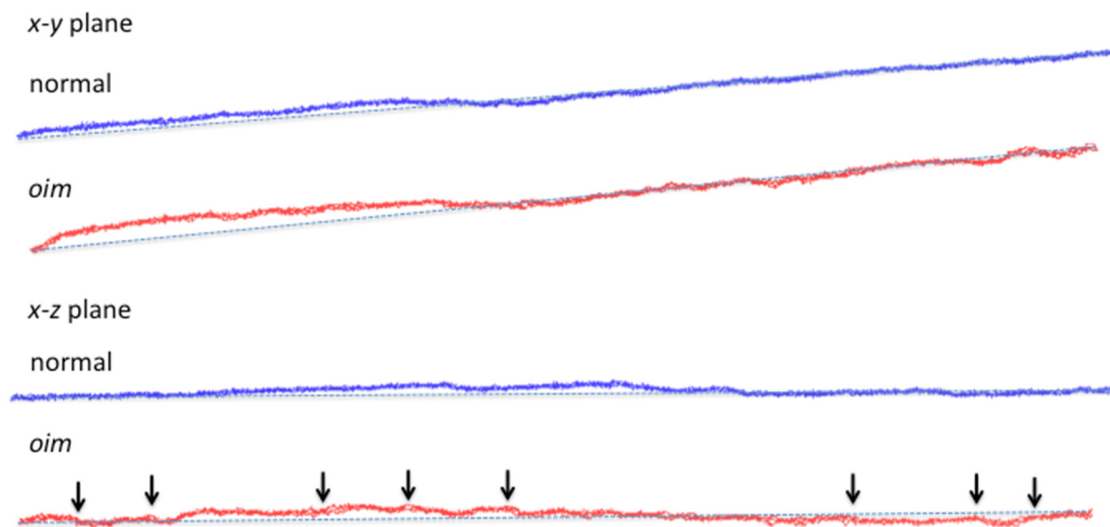


Figure S2. Molecular modeling of $+/+$ and oim/oim collagen fibrils: a direct comparison of the structures of normal and oim/oim collagen molecules. The dashed lines indicate the end-to-end distance of the collagen molecules. The oim/oim collagen molecule has more kinks (mostly in the gap region), which lead to the increase of lateral distance and the reduction of modulus based on the lateral compression test with no crosslinks on dry collagen fibril.

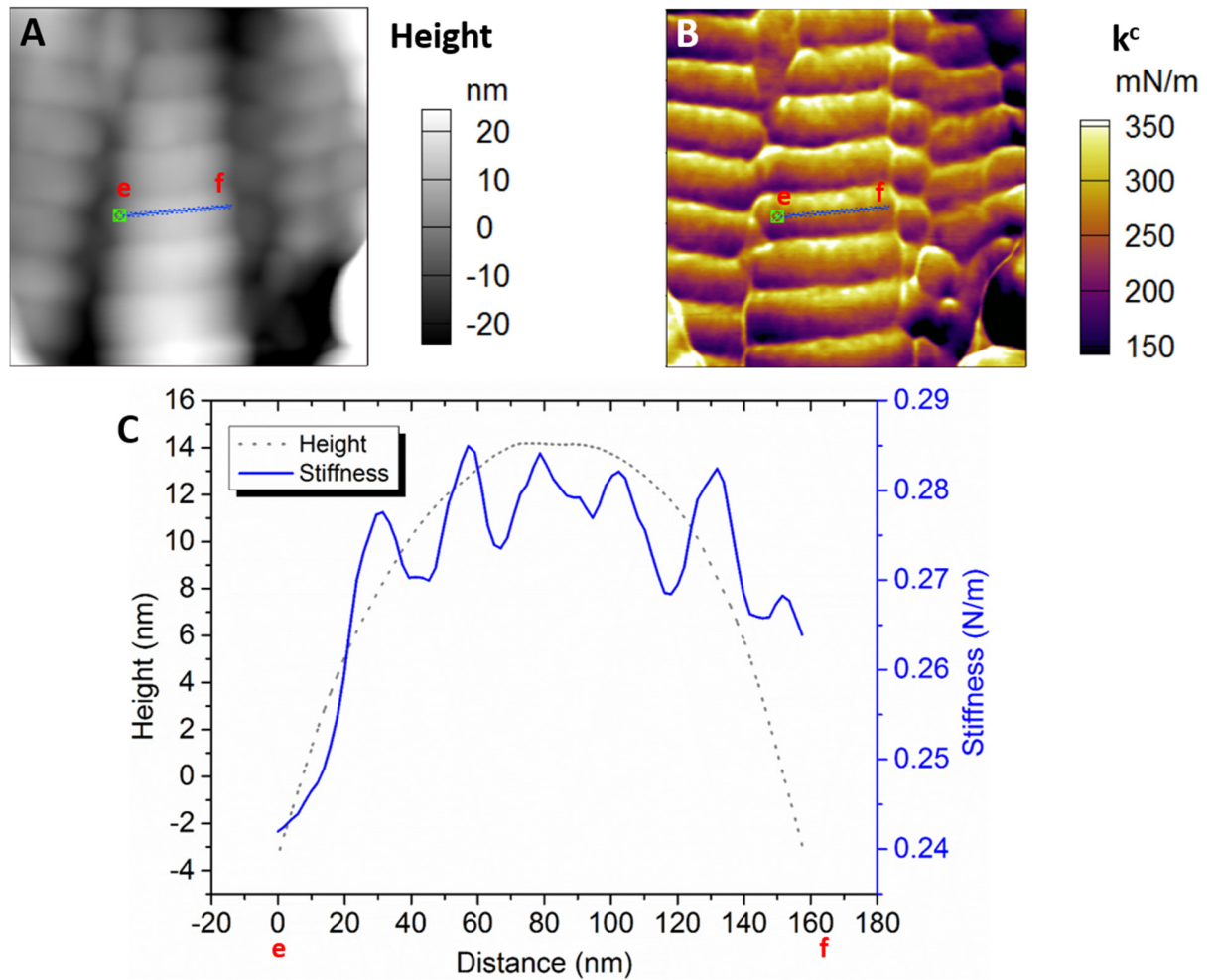


Figure S3. Dual-frequency AFM images of +/+ collagen fibers, showing higher order features along the fiber length direction. ($0.5 \times 0.5 \mu\text{m}^2$, 256×256 pixels). (A) Topography. (B) Stiffness mapping. (C) Stiffness data profile along the line e-f with corresponding height profile.

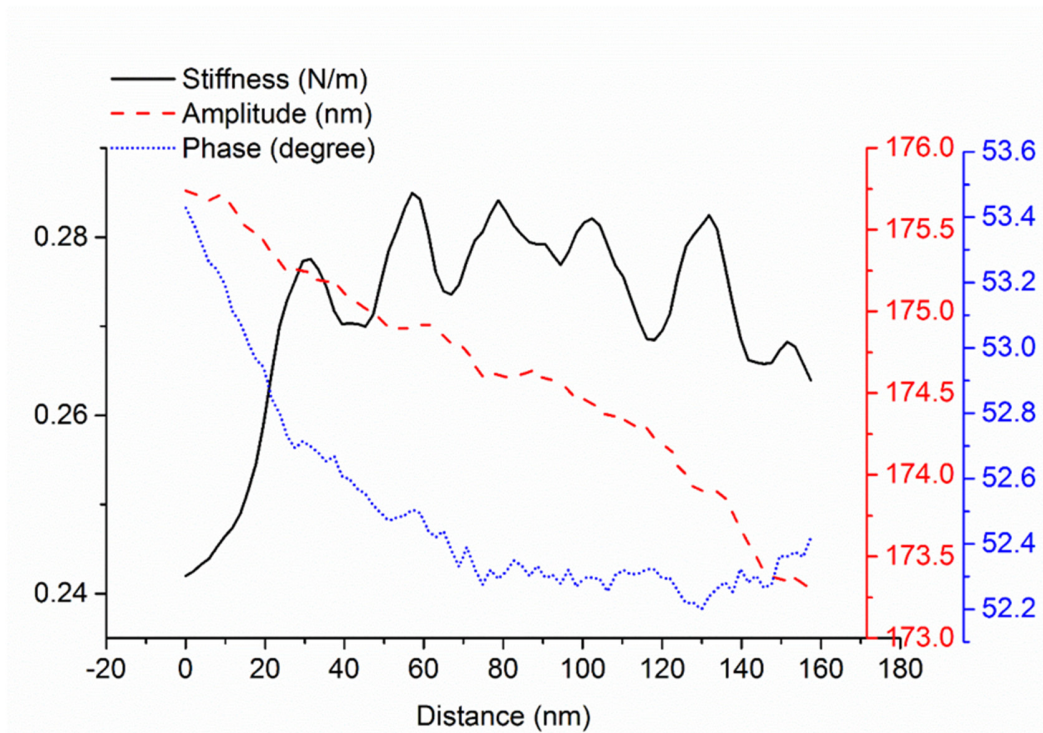


Figure S4. Sensitivity comparison among stiffness, amplitude and phase images. The corresponding line profiles are plotted along line e-f in Fig. S3.

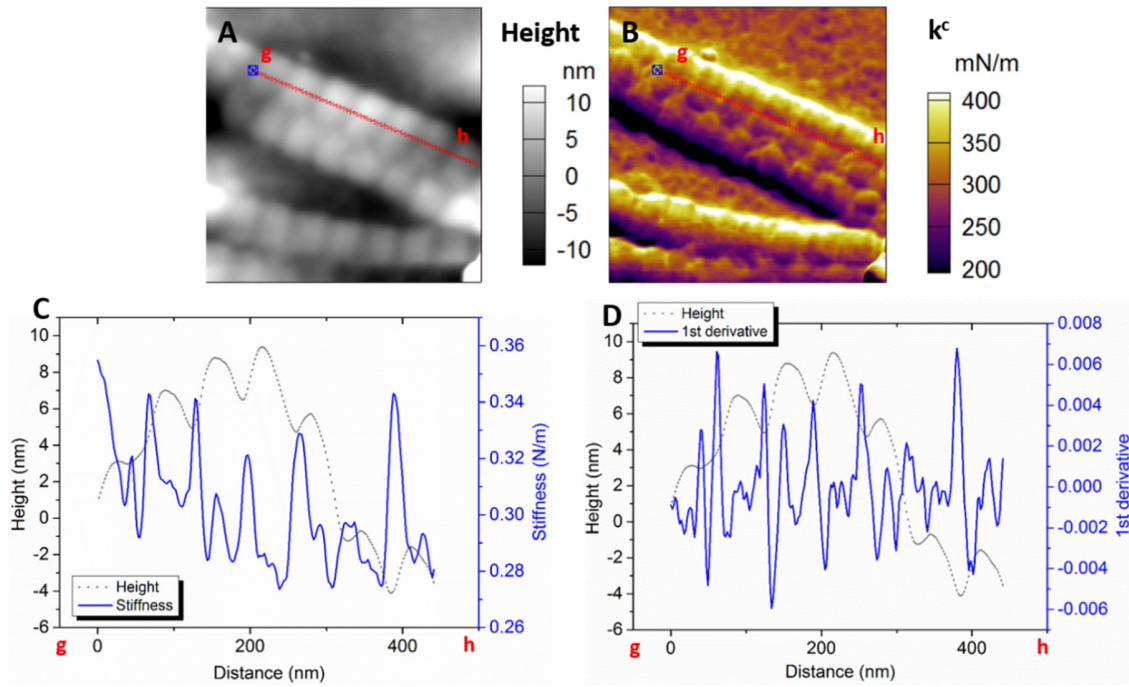


Figure S5. Dual-frequency AFM images and line profile of *oim/oim* collagen fiber ($0.5 \times 0.5 \mu\text{m}^2$, 256×256 pixels). (A) Topography image. (B) Stiffness mapping. (C) Stiffness and the corresponding topography profile along the line g-h. (D) First derivative of the stiffness profile.

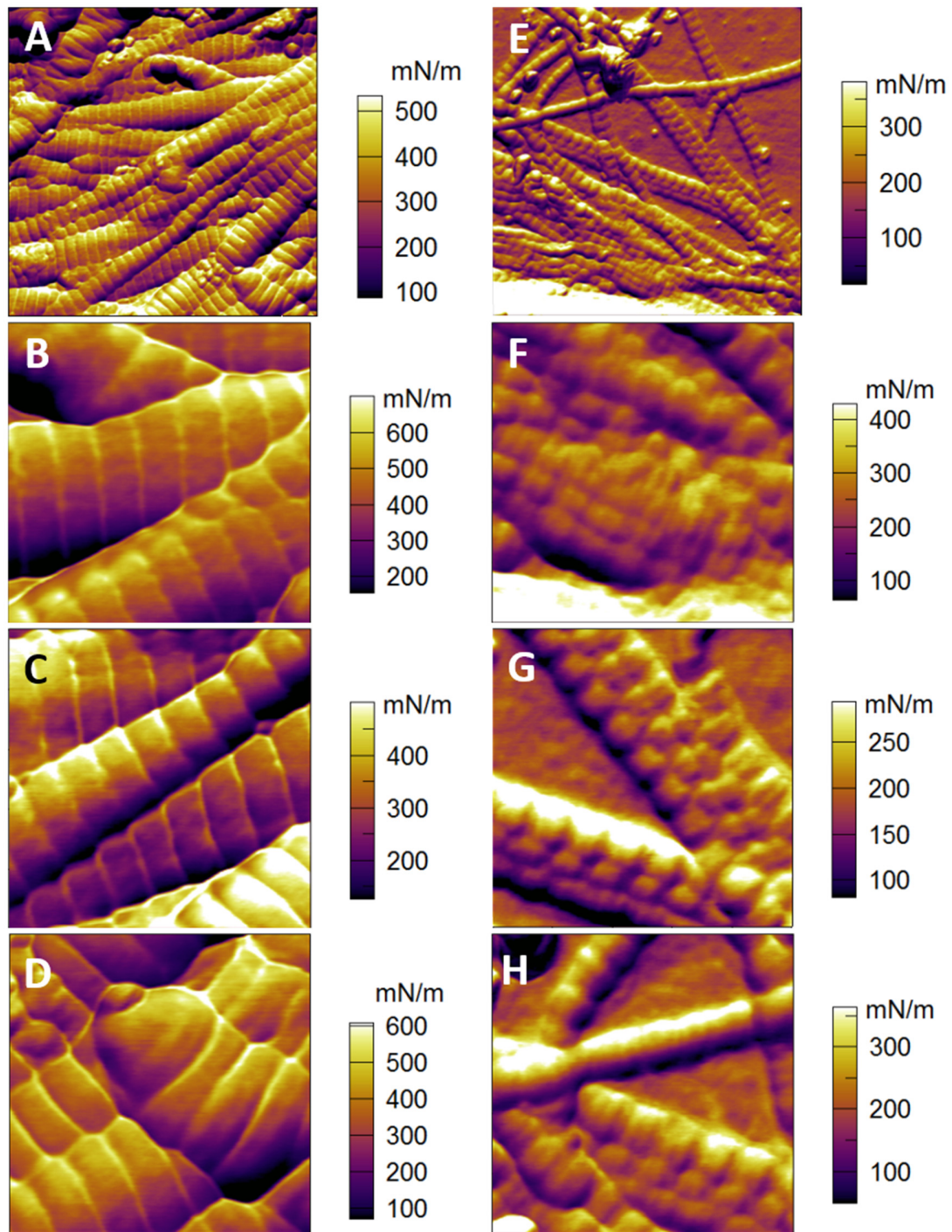


Figure S6. Original stiffness images of the histograms presented in Fig. 6. (A) to (D) +/- collagen fibers. (E) to (H) *oim/oim* collagen fibers. (A) and (E): $2 \times 2 \mu\text{m}^2$ with 512×512 pixels. The rest images: $0.5 \times 0.5 \mu\text{m}^2$ with 256×256 pixels. Only the fiber regions showing repeated units were counted in the histograms in Fig. 6.

References

- [1] D. Ebeling, S.D. Solares, Bimodal atomic force microscopy driving the higher eigenmode in frequency-modulation mode: Implementation, advantages, disadvantages and comparison to the open-loop case, *Beilstein J. Nanotechnol.* 4 (2013) 198-207.
- [2] G. Chawla, S.D. Solares, Mapping of conservative and dissipative interactions in bimodal atomic force microscopy using open-loop and phase-locked-loop control of the higher eigenmode, *Appl. Phys. Lett.* 99 (2011) 074103.
- [3] S.M. Weis, J.L. Emery, K.D. Becker, D.J. McBride, J.H. Omens, A.D. McCulloch, Myocardial mechanics and collagen structure in the osteogenesis imperfecta murine (oim), *Circ. Res.* 87 (2000) 663-669.